

# Thermodynamic and transport properties of single-crystalline $UMGa_5$ ( $M=Fe, Co, Ni, Ru, Rh, Pd, Os, Ir, Pt$ )

N. O. Moreno, E. D. Bauer, J. L. Sarrao, M. F. Hundley, J. D. Thompson, and Z. Fisk\*  
*Los Alamos National Laboratory, Los Alamos, New Mexico 87545, USA*

(Received 21 September 2004; revised manuscript received 18 May 2005; published 15 July 2005)

We report the results of magnetic susceptibility, specific heat, and electrical resistivity measurements on  $UMGa_5$  ( $M=Fe, Co, Ni, Ru, Rh, Pd, Os, Ir, Pt$ ) single crystals. Antiferromagnetic ordering was observed for  $M=Ni, Pd,$  and  $Pt$ , with ordering temperatures  $T_N=80$  K, 28 K, and 23.5 K, respectively. For the  $UMGa_5$  compounds with transition metals from the Fe and Co columns, itinerant paramagnetic behavior is observed. The evolution of this behavior is discussed in terms of  $f$ -ligand interaction with an emphasis on the role played by  $f$ - $d$  hybridization.

DOI: [10.1103/PhysRevB.72.035119](https://doi.org/10.1103/PhysRevB.72.035119)

PACS number(s): 75.20.Hr, 71.20.Lp, 71.27.+a

## I. INTRODUCTION

In the last several years, considerable attention has been dedicated to the interesting physical properties of the  $CeMIn_5$  ( $M=Rh, Ir, Co$ ) compounds.<sup>1–3</sup> These heavy fermion compounds display a rich variety of ground states including unconventional superconductivity, antiferromagnetism, and non-Fermi liquid behavior. Further, pressure-dependent and doping-dependent studies have revealed extremely rich phase diagrams that include the microscopic coexistence of superconductivity and magnetism.<sup>4–7</sup> Quite recently, superconductivity has also been reported in isostructural  $PuCoGa_5$  and  $PuRhGa_5$ .<sup>8,9</sup> Although less is known about these plutonium-based materials, the underlying physics appears to be similar<sup>10</sup> to that of  $CeMIn_5$  and, in particular, seems to rely on the existence of at least partially localized  $f$  electrons.<sup>11–13</sup>

A family of uranium-based analogues of  $CeMIn_5$  and  $PuMGa_5$  was reported some time ago.<sup>14</sup>  $UMGa_5$  crystallizes in the same tetragonal  $HoGoGa_5$ -type structure as the Ce and Pu variants for  $M=Fe, Co, Ni, Ru, Rh, Pd, Os, Ir, Pt$ . The observed physical properties, however, indicate itinerant  $f$ -electron behavior rather than localized behavior.<sup>15–18</sup> It has been suggested that the properties of  $CeMIn_5$  derive from constructing a layered variant of  $CeIn_3$ , which displays local-moment antiferromagnetism at ambient pressure.<sup>19</sup> At least qualitatively, the same argument can be made for  $UMGa_5$  because  $UGa_3$  displays itinerant  $f$ -electron behavior and orders antiferromagnetically near 80 K with only a weakly temperature-dependent magnetic susceptibility.<sup>20</sup>

The initial description of the  $UMGa_5$  compounds reported only a structural determination and magnetic susceptibility data at temperatures above 80 K on principally polycrystalline samples.<sup>14</sup> Subsequent studies have revealed that  $UNiGa_5$ ,  $UPtGa_5$ , and  $UPdGa_5$  order antiferromagnetically;<sup>21–23</sup> whereas, itinerant paramagnetic behavior is observed for the  $UMGa_5$  materials with other transition metals. Significant recent effort has been devoted to understanding the nature of the ordered compounds as well as to the evolution of the Fermi surface across many of these compounds as a function of transition metal.<sup>17,18,21,23,24</sup>

Here, we present a comprehensive study of magnetic susceptibility, specific heat, and electrical resistivity proper-

ties on the complete set of  $UMGa_5$  ( $M=Fe, Co, Ni, Ru, Rh, Pd, Os, Ir, Pt$ ) compounds, with all measurements performed on single crystals. In addition, we present results obtained with a simple tight-binding model that provides semi-quantitative insights into the role of  $f$ -ligand hybridization effects in explaining both the evolution of  $T_N$  for the ordered magnetic systems and the evolution of the paramagnetic behavior in the nonmagnets.

## II. EXPERIMENTAL DETAILS

Single crystals of  $UMGa_5$  ( $M=Fe, Co, Ni, Ru, Rh, Pd, Os, Ir, Pt$ ) have been grown from excess gallium flux. Stoichiometric ratios of U and  $M$  together with excess Ga were loaded into an alumina crucible and sealed inside an evacuated quartz ampoule. The molar ratio of the Ga flux to  $UMGa_5$  was 15:1. The mixture was heated to 1100 °C, allowed to equilibrate for 4 h and then cooled at 4 °C/h to 600 °C. At this point, the excess Ga flux was removed by centrifugation, yielding well-separated single crystals. X-ray powder diffraction measurements confirmed the  $HoCoGa_5$  structure with lattice parameters in agreement with previous results.<sup>14</sup>

The dc magnetic susceptibility  $\chi(T)=M/H$  measurements were performed by means of a commercial superconducting quantum interference device (SQUID) magnetometer (Quantum Design) in fields of 1 kOe in the temperature range 2–350 K. Heat capacity  $C_p(T)$  measurements were carried out using the thermal relaxation technique with a commercial calorimeter in the temperature range 0.5–300 K. The electrical resistivity  $\rho(T)$  was measured in a commercial <sup>4</sup>He cryostat, using a four-probe ac technique in the temperature range of 1.8–300 K under zero applied field. Bar-shaped samples were cut along the principal axes, and a current was applied along the [100] direction. Typical dimensions of resistivity samples were  $0.5 \times 0.5 \times 3.0$  mm<sup>3</sup>. The experimental error in the resistivity is less than 5%, due mainly to the uncertainty in the geometrical factor.

## III. RESULTS

X-ray diffraction measurements on crushed single crystals confirm that  $UMGa_5$  ( $M=Fe, Ni, Co, Ru, Os, Rh, Ir, Pd,$  and

TABLE I. Structural and physical properties of the  $UMGa_5$  compounds. Tetragonal lattice parameters ( $a, c$ ) and structural data ( $V, z_{Ga(2)}$ ) are obtained from x-ray and neutron diffraction measurements (Refs. 14 and 22) (except where otherwise noted). The electronic specific heat coefficient  $\gamma$  and phonon coefficient  $\beta$  (and corresponding Debye temperature  $\theta_D$ ) are obtained from fits of the low temperature specific heat. Néel temperature,  $T_N$ ; residual resistivity;  $\rho_0$ ;  $T^2$  coefficient of the electrical resistivity,  $A$ ; electron-magnon and spin disorder scattering parameter,  $D$ ; energy gap,  $\Delta$  (see Sec. III B).

Compound	$a$ (Å)	$c$ (Å)	$V$ (Å) <sup>3</sup>	$z_{Ga(2)}$	$\gamma$ ( $\frac{mJ}{mol K^2}$ )	$\beta$ ( $\frac{mJ}{mol K^4}$ )	$\theta_D$ (K)	$T_N$ (K)	$\rho_0$ ( $\mu\Omega cm$ )	$A$ ( $\frac{\mu\Omega cm}{K^2}$ )	$D$ ( $\mu\Omega cm$ )	$\Delta/k_B$ (K)	Ref.
UFeGa <sub>5</sub>	4.261	6.734	122.3	0.3082 <sup>a</sup>	37	0.299	357		0.8	0.0013			14
URuGa <sub>5</sub>	4.312	6.800	126.5	0.306 <sup>b</sup>	32	0.358	336		17.6	0.0172			14
UOsGa <sub>5</sub>	4.318	6.813	127.0	0.302 <sup>c</sup>	44	0.460	309		8.0	0.0022			14
UCoGa <sub>5</sub>	4.2357	6.7278	120.7	0.3082	21	0.216	398		22.0	0.0027			14
URhGa <sub>5</sub>	4.299	6.800	125.7	0.306 <sup>d</sup>	6	0.376	331		8.0	0.0009			9 and 14
UIrGa <sub>5</sub>	4.317	6.745	125.7	0.302 <sup>c</sup>	11	0.385	328						9, 14, and 29
UNiGa <sub>5</sub>	4.2380	6.7864	121.9	0.3074	53			80	1.8	0.0065	0.003	44	22
UPdGa <sub>5</sub>	4.3218	6.8637	128.2	0.2987	83			28	4.7	0.0565	0.321	131	22
UPtGa <sub>5</sub>	4.3386	6.8054	128.1	0.2964	64			23.5	6.7	0.0762	0.319	115	22

<sup>a</sup>Assumed to be the same as UCoGa<sub>5</sub>.

<sup>b</sup>Assumed to be the same as PuRhGa<sub>5</sub>.

<sup>c</sup>Assumed to be the same as PuIrGa<sub>5</sub>.

<sup>d</sup>Assumed to be the same as PuRhGa<sub>5</sub>.

<sup>e</sup>Assumed to be the same as PuIrGa<sub>5</sub>.

Pt) crystallizes in the tetragonal HoCoGa<sub>5</sub> structure type (space group  $P4/mmm$ ). Table I lists the room-temperature lattice parameters for all compounds.<sup>14,22</sup> It is worth noting that there is not a monotonic increase in the volume of the unit cell in the  $UMGa_5$  series with increasing atomic radius of the  $M$  metal. Thus, the variation in volume cannot be described solely by simple size (evolution down a column) or electron count (evolution along a row) effects.

The lattice parameters of  $UMGa_5$  imply a characteristic uranium-uranium spacing of 4.2–4.3 Å (the nearest-neighbor U—U distance is equal to  $a$ ). Using the Hill criterion, this would suggest localized  $5f$  behavior;<sup>25</sup> however, itinerant behavior is observed. This implies that rather than direct  $5f$ - $5f$  orbital interactions being dominant,  $5f$ -ligand interactions must contribute substantially in creating the observed itinerant behavior.<sup>15–18</sup>

It has been suggested that the  $d$ -bands associated with the transition metal  $M$  element are fully occupied in the  $UMGa_5$  materials with the hybridized U( $5f$ )-Ga( $4p$ ) conduction band giving rise to a relatively large density of states at the Fermi level and, hence, to itinerant magnetism.<sup>23</sup> However, recent neutron diffraction measurements<sup>22</sup> reveal different antiferromagnetic structures for  $M$ =Ni, Pd, Pt suggesting that the hybridization effects of the  $Uf$  and  $Md$  states have a significant influence on the nearest-neighbor interactions. This  $f$ - $d$  hybridization effect is observed, for instance, in the tetragonality  $t=(a-2z_{Ga(2)}c)/a$  vs  $M$  element of the  $UGa_3$  unit in  $UMGa_5$  as shown in Fig. 1. The smallest distortion ( $\sim 1.5\%$ ) of the  $UGa_3$  unit occurs for UNiGa<sub>5</sub> while the largest distortion ( $\sim 7\%$ ) is observed in UPtGa<sub>5</sub>. A linear decrease in the tetragonality  $t$  is found for the  $3d$  transition metal series ( $M$ =Fe, Co, Ni) while the  $5ds$  exhibit opposite behavior. The overall increase in magnitude of  $t$  progressing

from the  $3d$  to  $4d$  to  $5d$  elements (Fig. 1) is likely due to the larger extent of the heavier  $d$ -electron wave functions. It is also interesting to note the monotonic decrease of the Néel temperature  $T_N$  that occurs with increasing  $t$  in the sequence  $M$ =Ni, Pd, Pt.

### A. Paramagnetic properties of $UMGa_5$ ( $M$ =Fe, Ru, Os, Co, Rh, and Ir)

The magnetic susceptibility  $\chi(T)$  of the paramagnetic  $UMGa_5$  compounds ( $M$ =Fe, Ru, Os, Co, Rh, Ir) with  $H\parallel a$  is

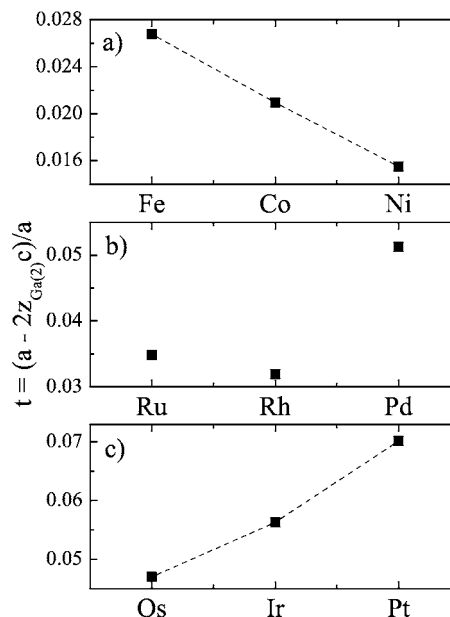


FIG. 1. Tetragonality  $t=(a-2z_{Ga(2)}c)/a$  of the  $UGa_3$  unit vs  $d$  element  $M$  of  $UMGa_5$ .

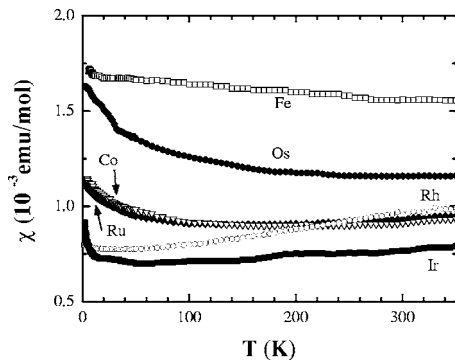


FIG. 2. Temperature dependence of the magnetic susceptibility  $\chi(T)$  of the paramagnetic  $UMGa_5$  ( $M=Fe, Ru, Os, Co, Rh, Ir$ ) compounds measured in a magnetic field  $H=1$  kOe.

shown in Fig. 2. Only a weak temperature dependence is observed consistent with enhanced paramagnetic behavior arising from itinerant  $f$  electrons as noted previously.<sup>14,15,18</sup> Low temperature values are of the order  $\chi_0 \sim 10^{-3}$  emu/mol. Data for field applied along the  $c$  axis are essentially identical, and no strong magnetic anisotropy is observed. The weak feature in the data at 30 K for  $M=Os$  is attributed to a small amount of an unknown impurity phase as there is no such anomaly in electrical resistivity or specific heat as discussed below.

The temperature-dependent electrical resistivity  $\rho(T)$  of  $UMGa_5$  ( $M=Fe, Co, Os, Ru, Rh, Ir$ ) is shown in Fig. 3. All exhibit metallic behavior except for  $UIrGa_5$  (inset of Fig. 3), whose temperature dependence has more structure. Both the increased magnitude of the resistivity and its temperature dependence suggest semimetallic behavior in  $UIrGa_5$ . For  $M \neq Ir$ , the electrical resistivity obeys a quadratic law  $\rho(T) = \rho_0 + AT^2$  below 20–40 K as shown in Fig. 4 with the parameters  $\rho_0$  and  $A$  listed in Table I. No traces of superconductivity nor any other evidence of long range order in the magnetic susceptibility or resistivity were observed between 1.8 K and 350 K.

The total specific heat divided by temperature  $C/T$  versus  $T^2$  is shown in Fig. 5.  $C/T$  at the lowest measured temperature, which we define as  $\gamma$ , varies from about 6 mJ/mol K<sup>2</sup> for  $M=Rh$  to almost 44 mJ/mol K<sup>2</sup> for  $M=Os$ . The specific heat of the  $UMGa_5$  compounds can be reasonably described

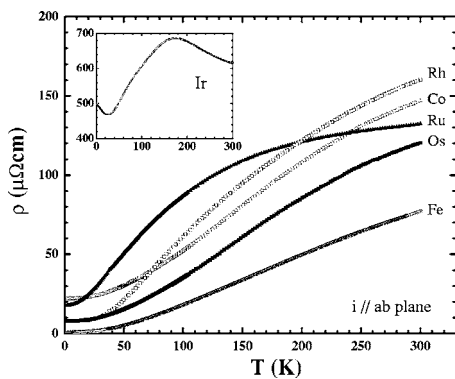


FIG. 3. Electrical resistivity  $\rho(T)$  of  $UMGa_5$  compounds. Inset:  $\rho(T)$  of  $UIrGa_5$ .

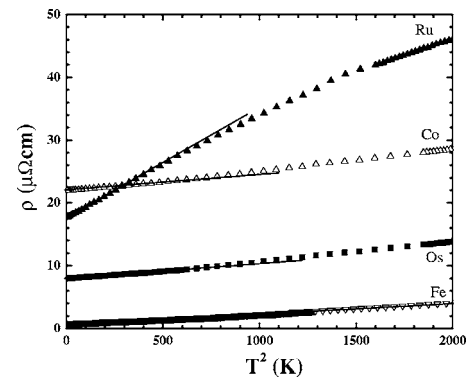


FIG. 4.  $\rho$  vs  $T^2$  for selected  $UMGa_5$  compounds. The lines are linear fits to the data.

by  $C/T = \gamma + \beta T^2$  at low  $T$ . Fitted values of  $\gamma$  and  $\beta$  (and the related Debye temperature) are listed in Table I.

### B. Antiferromagnetic properties of $UMGa_5$ ( $M=Ni, Pd$ , and Pt)

We now turn to the  $UMGa_5$  compounds that order magnetically. Recent neutron scattering studies<sup>17,22,23</sup> of  $UMGa_5$  ( $M=Ni, Pd$ , and Pt), show that in  $UNiGa_5$ , the adjacent uranium spins are oppositely aligned similar to  $UGa_3$  (Ref. 27) with an ordered moment of  $0.75-0.9\mu_B/U$ . On the other hand, the magnetic moments of uranium atoms in  $UPtGa_5$  and  $UPdGa_5$  are aligned in ferromagnetic sheets in the  $ab$  plane and stacked antiparallel along the  $c$  axis with an ordered moment of  $0.2-0.3\mu_B/U$  and  $0.34\mu_B/U$ , respectively.<sup>17,22,23</sup>

Figure 6 presents the temperature dependence of the magnetic susceptibility  $\chi(T)$  of single crystals of  $UNiGa_5$ ,  $UPtGa_5$ , and  $UPdGa_5$  for magnetic fields applied parallel and perpendicular to the  $c$  axis. For the Ni and Pd variants, the susceptibility is weakly temperature dependent displaying a peak at  $T_N=80$  K ( $UNiGa_5$ ) and  $T_N=28$  K ( $UPdGa_5$ ). The temperature-dependent magnetic susceptibility of  $UNiGa_5$  [Fig. 6(a)] resembles that of the itinerant antiferromagnet  $UGa_3$  ( $T_N=68$  K).<sup>26</sup> Figure 6(c) displays  $\chi(T)$  of  $UPtGa_5$ , which exhibits a peak at 26 K, but the Néel temperature is better defined as the maximum of  $d(\chi T)/dT$  (not shown), which occurs at  $T_N=23.5$  K. This value corresponds

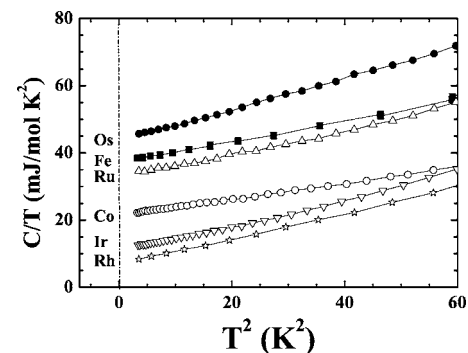


FIG. 5. Specific heat divided by temperature  $C/T$  vs  $T^2$  for  $UMGa_5$  compounds.

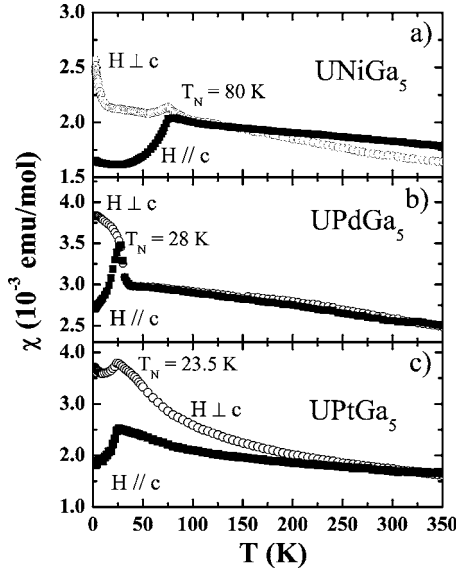


FIG. 6.  $\chi(T)$  of antiferromagnetic (a) UNiGa<sub>5</sub>, (b) UPdGa<sub>5</sub>, and (c) UPtGa<sub>5</sub>, measured at  $H=1$  kOe.

well with the anomaly in the specific heat discussed below. UPtGa<sub>5</sub> displays behavior closer to that expected for localized  $5f$  electrons, but a high temperature fit of the data to the Curie-Weiss law yields values of  $\mu_{eff}=1.84\mu_B$  and  $\theta=-133$  K ( $\mu_{eff}=\mu_B$ ,  $\theta=-387$  K) for field parallel (perpendicular) to the  $c$  axis. These values of  $\mu_{eff}$  are much smaller than the expected values for the  $5f^2$  or  $5f^3$  configurations of uranium ( $3.58$  or  $3.62\mu_B$ ), again suggesting strong hybridization of the  $5f$  electrons with the conduction electrons.

The magnetization  $M(H)$  data at  $T=2$  K in the principal directions of  $UMGa_5$  ( $M=Ni, Pd, Pt$ ) are shown in Fig. 7. The curves are typical of antiferromagnets and the anisotropy is modest ( $M_{ab}/M_c \sim 1.1-2$ ) in the antiferromagnetic (AFM) state, generally consistent with previous

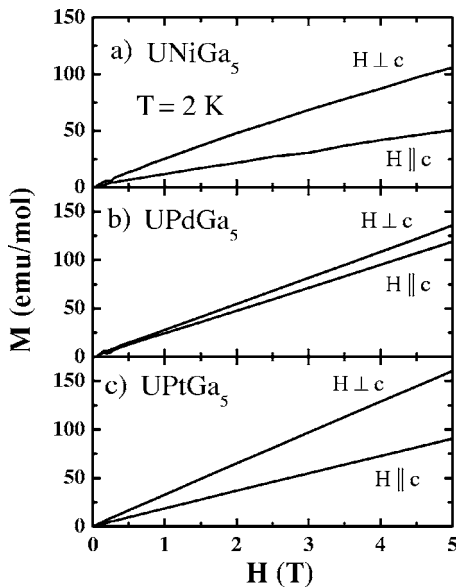


FIG. 7.  $M$  vs  $H$  with  $H\parallel c$  and  $H\perp c$  of antiferromagnetic (a) UNiGa<sub>5</sub>, (b) UPdGa<sub>5</sub>, and (c) UPtGa<sub>5</sub>, measured at  $T=2$  K.

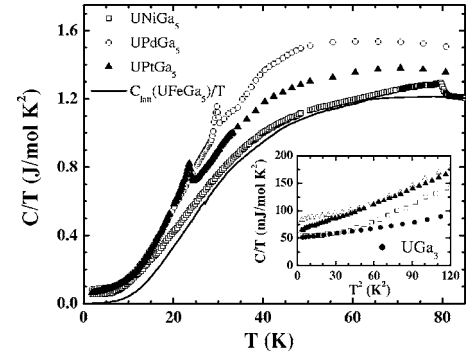


FIG. 8.  $C/T$  vs  $T$  for  $UMGa_5$  ( $M=Ni, Pd, Pt$ ) along with  $C_{lat}/T$  of  $UFeGa_5$  as discussed in the text. Inset:  $C(T)/T$  vs  $T^2$  of  $UMGa_5$  ( $M=Ni, Pd, Pt$ ) and  $UGa_3$  (Ref. 20). The lines are linear fits to the data.

reports.<sup>17,21,23</sup> However, the near isotropy of the  $M(H)$  curves of UPdGa<sub>5</sub> is somewhat different than found previously.<sup>23</sup> The magnetization in the  $ab$  plane is always largest, suggesting that it is easier to cant the moments that lie along the  $c$  axis in all three compounds<sup>17,22,23</sup> into the  $ab$  plane than to rotate them to all align along the  $c$  axis. A similar situation arises in CeRhIn<sub>5</sub>, except that the anisotropy is reversed (i.e.,  $M_c > M_{ab}$ ), since the moments lie in the  $ab$  plane and are spirally modulated along the  $c$  axis with an ordering wave vector  $\mathbf{Q}=(1/2, 1/2, 0.297)$ .<sup>28</sup> In localized systems containing uranium, the magnetization is expected to saturate to a value  $\mu_{sat}=3.28\mu_B$  ( $3.2\mu_B$ ) for  $U^{3+}$  ( $U^{4+}$ ) at modest fields (assuming  $L$ - $S$  coupling). However, the magnetization only reaches  $\sim 150$  emu/mol ( $0.027\mu_B/U$ ) at 2 K in the antiferromagnetic state (Fig. 7) with no tendency toward saturation. Indeed,  $M(H)$  for UPtGa<sub>5</sub> does not saturate even in magnetic fields of 50 T reaching a value of only  $0.4\mu_B/U$  at 4.2 K for  $H\parallel[100]$ , indicating itinerant antiferromagnetism.<sup>21</sup>

Figure 8 shows specific heat data for  $UMGa_5$  ( $M=Ni, Pd, Pt$ ) and  $UGa_3$ .<sup>20</sup> The antiferromagnetic transition in UNiGa<sub>5</sub>, UPdGa<sub>5</sub>, and UPtGa<sub>5</sub> is observed at  $T_N=80$  K, 28 K, and 23.5 K, respectively. The temperature dependence of specific heat for  $T < 8$  K can be described as  $C/T=\gamma + \beta T^2$  for each compound. A rough estimate of  $\gamma$  can be made by examining the low-temperature behavior of  $C/T$  vs  $T^2$  as shown in inset of Fig. 8. The low-temperature extrapolation yields  $\gamma$  values of 47, 83, and 62 mJ/mol K<sup>2</sup> (see Table I). A rough estimate of the magnetic entropy released below the magnetic transition was obtained using the following procedure, since a nonmagnetic analog  $ThMGa_5$  does not exist. First, the electronic contribution  $\gamma T$  was subtracted from the specific heat of  $UMGa_5$  ( $M=Ni, Pd, Pt$ ) using the values of  $\gamma$  listed in Table I. After this subtraction, the lattice contribution of the paramagnetic compounds of  $UFeGa_5$  ( $UIrGa_5$ ) were subtracted from the remaining  $5f$  contribution to the specific heat of UNiGa<sub>5</sub> (UPdGa<sub>5</sub> and UPtGa<sub>5</sub>) (Fig. 8), yielding the magnetic specific heat  $C_{mag}$ . The magnetic entropy in the AFM state was then determined from  $S_{mag}(T_N)=\int_0^{T_N}(C_{mag}/T)dT$ , yielding  $S_{mag} \sim 0.7R \ln(2)$ ,  $0.4R \ln(2)$ , and  $0.3R \ln(2)$  for UNiGa<sub>5</sub>, UPdGa<sub>5</sub>, and UPtGa<sub>5</sub>, respectively (with uncertainties of the order of 50%). These relatively low values of the magnetic entropy,



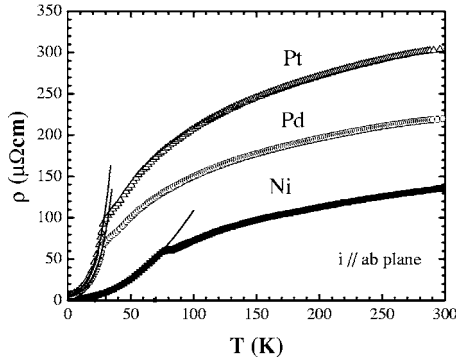


FIG. 9.  $\rho(T)$  of  $UMGa_5$  ( $M=Ni, Pd, \text{ and } Pt$ ) compounds. The lines are fits of Eq. (1) to the data.

considerably lower than  $R \ln(9)$  or  $R \ln(10)$  as expected for a localized  $U^{4+}$  or  $U_{3+}$  ion, respectively, clearly indicate itinerant  $5f$  magnetism in these compounds.

The temperature dependence of the electrical resistivity  $\rho(T)$  for  $UMGa_5$  ( $M=Ni, Pd, \text{ and } Pt$ ) is shown in Fig. 9. The data are consistent with previous reports.<sup>17,21,23</sup> The resistivity displays a clear signature of the Néel temperature (80 K, 28 K, and 23.5 K for  $M=Ni, Pd, \text{ and } Pt$ , respectively). At low temperatures, the electrical resistivity can be well fit by the equation

$$\rho(T) = \rho_0 + AT^2 + DT\Delta^{-1}(1 + 2T\Delta^{-1})e^{-\Delta/T}, \quad (1)$$

which describes the scattering due to an energy gap in the magnon dispersion relation.<sup>30–32</sup> In Eq. (1),  $D$  involves the electron-magnon and the spin-disorder scattering and  $\Delta$  is the magnitude of the gap. The lines in Fig. 9 are the best fit of Eq. (1) to the experimental data ( $\rho_0$  has been fixed to the value obtained from fits of  $\rho(T) = \rho_0 + AT^2$  at the lowest temperature). The value of  $A$  in this group of antiferromagnetic compounds is enhanced relative to their nonmagnetic counterparts. To further test the intrinsic nature of the enhancement of  $A$ , we have compared it to the measured values of  $\gamma$  using the Kadowaki-Woods relation.<sup>33</sup> Although the validity of this universal behavior is questionable in magnetically ordered materials, where the anisotropy of the magnetic structure and magnetic excitations can lead to different  $A$  values in different directions, we find that the experimental  $A/\gamma^2$  values of  $UNiGa_5$ ,  $UPdGa_5$ , and  $UPtGa_5$  are close to this universal ratio  $A/\gamma^2 = 1 \times 10^{-5} \mu\Omega \text{ cm} (\text{mol K/mJ})^2$ .

#### IV. DISCUSSION

The magnetism in uranium intermetallic compounds is usually governed by two mechanisms: first, the direct overlap of  $5f$  wave functions of neighboring U atoms, which explains the importance of the inter-Uranium spacing  $d_{U-U}$  as proposed by Hill,<sup>25</sup> and second, the  $5f$ -ligand hybridization, which is particularly important in compounds with larger U—U distances. Isostructural groups of compounds are well suited for systematic studies of these mechanisms because the local geometry of the U ion is unchanged.

As discussed above and in Refs. 15–17, the Hill criterion does not provide an accurate description of the behavior of

$UMGa_5$ . A reasonable and simple estimate of the strength of the  $5f$ -ligand hybridization in a series of isostructural compounds may be obtained employing the method developed by Straub and Harrison.<sup>34,35</sup> A tight-binding approximation is used to obtain the contribution to the hybridization of the U atoms and the X ligands

$$V_{UX} = \left( \frac{\eta_{fl} \hbar^2}{m_e} \right) \left[ \frac{\sqrt{r_{Uf}^3 r_{Xl}^{2l-1}}}{d_{U-X}^{l+4}} \right], \quad (2)$$

where  $r_{Xl}$  is the radius of the electronic shell of atom X with angular momentum  $l$ ,  $d_{U-X}$  is the bond length between the U atoms and the X ligands, and  $\eta_{fl}$  is a coefficient that depends only on  $l$  and the bond symmetry ( $\sigma$  bonds assumed). For simplicity, the total hybridization is obtained by summing the contributions of only the nearest neighbors. In the  $HoCoGa_5$  structure, the uranium atoms have the following coordination: four nearest U neighbors in the  $ab$  plane at a distance,  $d_{U-U} = a$ ; each U atom has two transition metal nearest neighbors along the  $c$  axis at a distance,  $d_{U-M} = c/2$ , and finally U has four in-plane Ga(1) and eight out-of-plane Ga(2) nearest neighbors at distances  $d_{U-Ga(1)} = a\sqrt{2}/2$  and  $d_{U-Ga(2)} = \sqrt{(a/2)^2 + (z_{Ga(2)}c)^2}$ , respectively. Using the structural parameters listed in Table I, the results of the calculations are given in Table II.

Examination of Table II reveals that the hybridization is dominated by the hybridization between the  $Uf$  states and the  $Gap$  states; the values are comparable to those of  $UGa_3$  suggesting that this  $f$ - $p$  hybridization may be responsible for the itinerant behavior observed in  $UMGa_5$ . However, the largest relative changes occur in  $V_{fd}$  (as much as 60%) compared to only 10% changes in the other contributions, stressing the importance of the  $f$ - $d$  hybridization on the physical properties of  $UMGa_5$ . It appears that the  $f$ - $d$  hybridization is dominated by  $d$  band filling effects as there is a systematic decrease in  $V_{fd}$  with increasing  $d$ -electron count (in a given row) while  $d_{U-M}$  remains essentially unchanged. The decrease in  $f$ - $d$  hybridization likely results from the larger separation of the  $d$  band relative to the Fermi level  $E_F$  as more  $d$  electrons are added. In addition, the  $f$ - $d$  hybridization increases as the size of the  $M$  atom increases in  $UMGa_5$ , i.e., as one moves down a column in the Periodic Table, the effective  $d$  shell radius increases for the heavier transition metals. In the Doniach model, the sensitive balance between the Ruderman-Kittel-Kasuya-Yosida (RKKY) interaction and the Kondo interaction, which are governed by a single energy scale (i.e., the hybridization strength  $\mathcal{J}$ ), leads to either a magnetic or nonmagnetic ground state. For small  $\mathcal{J}$ , the RKKY interaction dominates due to the algebraic dependence on  $\mathcal{J}$  [ $T_{RKKY} \sim \mathcal{J}^2 N(E_F)$ , where  $N(E_F)$  is the density of states at the Fermi level] favoring a magnetically ordered ground state; for sufficiently large hybridization strength, the exponential dependence of the Kondo temperature with  $\mathcal{J}$  [ $T_K \sim \exp[-1/\mathcal{J}N(E_F)]$ ] suppresses magnetic order. The competition of these two interactions results in an asymmetric “bell-shaped” curve of  $T_{mag}$  vs  $\mathcal{J}$  known as the Doniach diagram.<sup>36</sup> The increased  $f$ - $d$  hybridization in the series Ni—Pd—Pt is consistent with the decrease of  $T_N$  (=80 K, 28 K, and 23.5 K for Ni, Pd, and Pt, respectively) within the

TABLE II. Hybridization energy of  $UMGa_5$ ,  $PuCoGa_5$ ,  $PuRhGa_5$ , and  $CeMIn_5$  compounds using the structural parameters given in Table I and literature (see Refs. 9, 14, and 22) values.  $V_{UX}$  is calculated from Eq. (2) and includes the sum over nearest neighbors for a particular ligand  $X$ . The total hybridization  $V_{total}$  of the U atoms with the ligand atoms is obtained by summing over all contributions  $V_{UX}$ .

Compound	$d_{U-U}(\text{\AA})$	$d_{U-M}(\text{\AA})$	$d_{U-Ga(1)}(\text{\AA})$	$d_{U-Ga(2)}(\text{\AA})$	$V_{UU}$ (meV)	$V_{UM}$ (meV)	$V_{UGa(1)}$ (meV)	$V_{UGa(2)}$ (meV)	$V_{total}$ (eV)
UFeGa <sub>5</sub>	4.261	3.3670	3.0158	2.9758	141.7	68.2	1969.1	4210.9	6.389
URuGa <sub>5</sub>	4.312	3.4000	3.0490	2.9963	131.3	117.3	1864.3	4068.2	6.181
UOsGa <sub>5</sub>	4.318	3.4065	3.0533	2.9824	130.0	121.3	1851.4	4164.2	6.266
UCoGa <sub>5</sub>	4.2357	3.3639	2.9951	2.9639	148.8	61.4	2038.3	4295.7	6.544
URhGa <sub>5</sub>	4.299	3.4000	3.0399	2.9917	134.1	105.3	1892.6	4100.1	6.232
UIrGa <sub>5</sub>	4.317	3.3725	3.0526	2.9679	130.2	118.4	1853.5	4266.9	6.368
UNiGa <sub>5</sub>	4.2380	3.3932	2.9967	2.9736	148.2	51.7	2032.8	4226.3	6.459
UPdGa <sub>5</sub>	4.3128	3.4319	3.0560	2.9787	129.2	99.5	1843.2	4189.9	6.261
UPtGa <sub>5</sub>	4.3386	3.4027	3.0679	2.9622	125.8	109.7	1807.8	4308.1	6.351
PuCoGa <sub>5</sub>	4.2354	3.3965	2.9946	2.9768	94.8	45.8	1627.3	3353.1	5.121
PuRhGa <sub>5</sub>	4.3012	3.4280	3.0413	3.0043	85.1	79.3	1506.3	3202.3	4.873
PuIrGa <sub>5</sub>	4.324	3.4085	3.0575	2.9854	81.9	87.6	1466.6	3305.1	4.941
UGa <sub>3</sub>	4.29		3.0335		204.1		5737.7		5.942

Doniach framework assuming that  $UNiGa_5$  is located at (or to the right of) the maximum of the  $T_{mag}(\mathcal{J})$  curve. A number of other families of isostructural compounds, such as  $UT_2X_2$ ,  $UTX$ , and  $U_2T_2X$  ( $T$ =transition metal;  $X$ =Si, Ge),<sup>37-39</sup> display similar behavior and stress the importance of  $f$ - $d$  hybridization in determining the physical properties. For instance, all of the  $UT_2X_2$  materials can be placed on the Doniach diagram by considering the  $f$ - $d$  hybridization within the simple tight-binding framework discussed above, regardless of the type of magnetic order. A similar analysis of the  $UTX$  and  $U_2T_2X$  systems is consistent with the occurrence of magnetic or nonmagnetic ground states.<sup>38,39</sup>

The tight-binding analysis can be extended to include the isostructural  $PuMGa_5$  ( $M$ =Co, Rh, Ir) materials.  $PuCoGa_5$  exhibits superconductivity at  $T_c=18.5$  K; various thermodynamic measurements indicate a moderate quasiparticle mass enhancement of  $\gamma\sim 80$  mJ/mol K<sup>2</sup>. Superconductivity is also found in  $PuRhGa_5$  at  $T_c=8.7$  K, which has a slightly smaller Sommerfeld coefficient  $\gamma\sim 50$  mJ/mol K<sup>2</sup>.<sup>9</sup> In contrast, no superconductivity or magnetic order is observed in  $PuIrGa_5$  down to 1.4 K.<sup>29</sup> As in the case of the  $UMGa_5$  materials, the largest relative increase in hybridization is found in  $V_{fd}$  in  $PuMGa_5$ , consistent with the decrease in Sommerfeld coefficient; extension of this model to  $PuIrGa_5$  indicates an even smaller  $\gamma$  for this compound, in agreement with the small value of the  $T^2$  coefficient of the electrical

resistivity.<sup>29,33</sup> One might expect that  $V_{fd}$  may play a role in determining  $T_c$ , which varies by a factor of 2 between  $PuCoGa_5$  and  $PuRhGa_5$ ; however, it has recently been shown that structural tuning plays a more important role in the superconductivity of both  $PuMGa_5$  and the heavy-fermion  $CeMIn_5$  ( $M$ =Co, Rh, Ir) compounds.<sup>10,40</sup>

## V. SUMMARY

The physical properties of single crystals of  $UMGa_5$  are reported based on x-ray diffraction, magnetization, heat capacity, and electrical resistivity measurements.  $UMGa_5$  orders antiferromagnetically for  $M$ =Ni, Pd, and Pt, while for  $M$ =Fe, Ru, Os, Co, Rh, and Ir, itinerant paramagnetic behavior is observed. Although  $f$ - $p$  hybridization is by far the strongest matrix element,  $f$ - $d$  hybridization appears to play an important role in determining relative trends in these materials.

## ACKNOWLEDGMENTS

We thank P. G. Pagliuso and E. G. Moshopoulou for important contributions in the early stages of this investigation and S. B. Oseroff for helpful discussions. The work was performed under the auspices of the U.S. Department of Energy. E. D. B. thanks the G. T. Seaborg Institute for financial support.

\*Present address: Department of Physics, University of California, Davis, CA 95616, USA.

<sup>1</sup>H. Hegger, C. Petrovic, E. G. Moshopoulou, M. F. Hundley, J. L. Sarrao, Z. Fisk, and J. D. Thompson, Phys. Rev. Lett. **84**, 4986 (2000).

<sup>2</sup>C. Petrovic, P. G. Pagliuso, M. F. Hundley, R. Movshovich, J. L. Sarrao, J. D. Thompson, Z. Fisk, and P. Monthoux, J. Phys.: Condens. Matter **13**, L337 (2001).

<sup>3</sup>C. Petrovic, R. Movshovich, M. Jaime, P. G. Pagliuso, M. F. Hundley, J. L. Sarrao, Z. Fisk, and J. D. Thompson, Europhys.

- Lett. **53**, 354 (2001).
- <sup>4</sup>P. G. Pagliuso, R. Movshovich, A. D. Bianchi, M. Nicklas, N. O. Moreno, J. D. Thompson, M. F. Hundley, J. L. Sarrao, and Z. Fisk, *Physica B* **312–313**, 129 (2001).
  - <sup>5</sup>V. S. Zapf, E. J. Freeman, E. D. Bauer, J. Petricka, C. Sirvent, N. A. Frederick, R. P. Dickey, and M. B. Maple, *Phys. Rev. B* **65**, 014506 (2001).
  - <sup>6</sup>V. A. Sidorov, M. Nicklas, P. G. Pagliuso, J. L. Sarrao, Y. Bang, A. V. Balatsky, and J. D. Thompson, *Phys. Rev. Lett.* **89**, 157004 (2002).
  - <sup>7</sup>M. Nicklas, V. A. Sidorov, H. A. Borges, P. G. Pagliuso, C. Petrovic, Z. Fisk, J. L. Sarrao, and J. D. Thompson, *Phys. Rev. B* **67**, 020506(R) (2002).
  - <sup>8</sup>J. L. Sarrao, L. A. Morales, J. D. Thompson, B. L. Scott, G. R. Stewart, F. Wastin, J. Rebizant, P. Boulet, E. Collneau, and G. H. Lander, *Nature (London)* **420**, 297 (2002).
  - <sup>9</sup>F. Wastin, P. Boulet, J. Rebizant, E. Collneau, and G. H. Lander, *J. Phys.: Condens. Matter* **15**, S2279 (2003).
  - <sup>10</sup>E. D. Bauer, J. D. Thompson, J. L. Sarrao, L. A. Morales, F. Wastin, J. Rebizant, J. C. Griveau, P. Javorsky, P. Boulet, E. Colineau, G. H. Lander, and G. R. Stewart, *Phys. Rev. Lett.* **93**, 147005 (2004).
  - <sup>11</sup>I. Opahle and P. M. Oppeneer, *Phys. Rev. Lett.* **90**, 157001 (2003).
  - <sup>12</sup>T. Maehira, T. Hotta, K. Ueda, and A. Hasegawa, *Phys. Rev. Lett.* **90**, 207007 (2003).
  - <sup>13</sup>J. J. Joyce, J. M. Wills, T. Durakiewicz, M. T. Butterfield, E. Guziewicz, J. L. Sarrao, L. A. Morales, A. J. Arko, and O. Eriksson, *Phys. Rev. Lett.* **91**, 176401 (2003).
  - <sup>14</sup>Y. N. Grin, P. Rogl, and K. Heibl, *J. Less-Common Met.* **121**, 497 (1986).
  - <sup>15</sup>V. Sechovský, L. Havela, G. Schaudy, G. Hilscher, N. Pillmayr, P. Rogl, and P. Fischer, *J. Magn. Magn. Mater.* **104–107**, 11 (1992).
  - <sup>16</sup>M. Schönert, S. Corsépius, E.-W. Scheidt, and G. R. Stewart, *J. Alloys Compd.* **224**, 108 (1995).
  - <sup>17</sup>Y. Tokiwa, Y. Haga, E. Yamamoto, D. Aoki, N. Watanabe, R. Settai, T. Inoue, K. Kindo, H. Harima, and Y. Onuki, *J. Phys. Soc. Jpn.* **70**, 1744 (2001).
  - <sup>18</sup>Y. Tokiwa, T. Maehira, S. Ikeda, Y. Haga, E. Yamamoto, A. Nakamura, Y. Onuki, M. Higuchi, and A. Hasegawa, *J. Phys. Soc. Jpn.* **70**, 2982 (2001).
  - <sup>19</sup>E. G. Moshopoulou, Z. Fisk, J. L. Sarrao, and J. D. Thompson, *J. Solid State Chem.* **158**, 25 (2001).
  - <sup>20</sup>A. L. Cornelius, A. J. Arko, J. L. Sarrao, J. D. Thompson, M. F. Hundley, C. H. Booth, N. Harrison, and P. M. Oppeneer, *Phys. Rev. B* **59**, 14473 (1999), and references therein.
  - <sup>21</sup>Y. Tokiwa, S. Ikeda, Y. Haga, T. Okubo, T. Iizuka, K. Sugiyama, A. Nakamura, and Y. Onuki, *J. Phys. Soc. Jpn.* **71**, 845 (2002).
  - <sup>22</sup>K. Kaneko, N. Metoki, N. Bernhoeft, G. H. Lander, Y. Ishii, S. Ikeda, Y. Tokiwa, Y. Haga, and Y. Onuki, *Phys. Rev. B* **68**, 214419 (2003).
  - <sup>23</sup>S. Ikeda, N. Metoki, Y. Haga, K. Kaneko, T. D. Matsuda, A. Galatanu, and Y. Ōnuki, *J. Phys. Soc. Jpn.* **72**, 2622 (2003).
  - <sup>24</sup>S. Ikeda, Y. Tokiwa, T. Ōkubo, M. Yamada, T. D. Matsuda, Y. Inada, R. Settai, E. Yamamoto, Y. Haga, and Y. Ōnuki, *Physica B* **329–333**, 610 (2003).
  - <sup>25</sup>H. H. Hill, in *Plutonium and Other Actinides*, edited by W. N. Miner (AIME, New York, 1970), p. 2.
  - <sup>26</sup>K. G. Wilson, *Rev. Mod. Phys.* **47**, 773 (1975).
  - <sup>27</sup>A. Murasik, J. Leciejew, S. Ligenza, and A. Zygmunt, *Phys. Status Solidi A* **23**, K147 (1974).
  - <sup>28</sup>Wei Bao, P. G. Pagliuso, J. L. Sarrao, J. D. Thompson, Z. Fisk, J. W. Lynn, and R. W. Erwin, *Phys. Rev. B* **62**, R14621 (2000); *Phys. Rev. B* **63**, 219901(E) (2001); *Phys. Rev. B* **67**, 099903(E) (2003).
  - <sup>29</sup>J. C. Griveau, P. Boulet, F. Wastin, and J. Rebizant, *Physica B* **359**, 1093 (2005).
  - <sup>30</sup>K. Prokeš, T. Fujita, E. Brück, F. R. de Boer, and A. A. Menovsky, *Phys. Rev. B* **60**, R730 (1999).
  - <sup>31</sup>V. A. Sidorov, E. D. Bauer, N. A. Frederick, J. R. Jeffries, S. Nakatsuji, N. O. Moreno, J. D. Thompson, M. B. Maple, and Z. Fisk, *Phys. Rev. B* **67**, 224419 (2003).
  - <sup>32</sup>N. H. Andersen, in *Crystalline Field and Structural Effects in f-Electron Systems*, edited by J. E. Crow, R. P. Guertin, and T. W. Mihalisin (Plenum, New York, 1980), p. 373.
  - <sup>33</sup>K. Kadowaki and S. B. Woods, *Solid State Commun.* **58**, 307 (1986).
  - <sup>34</sup>G. K. Straub and W. A. Harrison, *Phys. Rev. B* **31**, 7668 (1985).
  - <sup>35</sup>W. A. Harrison and G. K. Straub, *Phys. Rev. B* **36**, 2695 (1987).
  - <sup>36</sup>S. Doniach, *Physica B & C* **91**, 231 (1977).
  - <sup>37</sup>J. A. Mydosh, T. Endstra, and G. J. Nieuwenhuys, in *Transport and Thermal Properties of f-Electron Systems*, edited by G. Oomi, H. Fujii and T. Fujita (Plenum Press, New York, 1993), pp. 93–102.
  - <sup>38</sup>A. M. Alsmadi, V. Sechovsky, A. H. Lacerda, K. Prokes, J. Kamarad, E. Brück, S. Chang, M. H. Jung, and H. Nakotte, *J. Appl. Phys.* **91**, 8123 (2002).
  - <sup>39</sup>K. Prokes, E. Brück, H. Nakotte, P. F. de Chatel, and F. R. de Boer, *Physica B* **206&207**, 8 (1995).
  - <sup>40</sup>J. L. Sarrao, E. D. Bauer, L. A. Morales, J. D. Thompson *Physica B* **359**, 1144 (2005)